ORIGINAL RESEARCH ARTICLE

Effect of Additives and Cl^- Ions on the Physical and Chemical Properties of Cobalt Deposits Obtained by Electrowinning

DANIELLE COSTAL DE CASTRO, IRANILDES DANIEL DOS SANTOS, REINER NEUMANN, PEDRO PAULO MEDEIROS RIBEIRO, and ACHILLES JUNQUEIRA BOURDOT DUTRA

The optimization of the cobalt electrowinning process is crucial to enhance the quality of metallic deposits, as cobalt plays a fundamental role in the manufacturing of high-tech materials. Thus, the effect of the additives sodium lauryl sulfate (SLS), boric acid, and Cl^- ions on the physical and chemical properties of cobalt deposits obtained by electrowinning are scarce in the literature. The present study investigated the effect of additive concentrations on current efficiency (CE), specific energy consumption (SEC), and the physical and chemical properties of cobalt deposits (crystalline phases, grain and crystallite sizes, morphology, purity, and microhardness) produced through electrodeposition tests in presence of a cobalt sulfate solution at 200 A m^{-2}, 60 °C, and pH 4. The results indicated that the presence of 0.05 g L^{-1} of SLS in the solution led to the best values for CE (95.5 pct) and SEC (1.80 kWh kg^{-1}), as well as the production of uniform deposits. Cracks were identified in the cross-sectional area of the metallic deposits under all evaluated conditions, with the detection of oxygen in these areas, except for Cl^- ions. Higher concentrations of SLS and boric acid resulted in the production of deposits with low microhardness and less fragility, attributed to the increased of crystallite and grain sizes. The predominant crystalline phase for all deposits was hexagonal close-packed (HCP), but the presence of SLS and Cl^- ions led to the rise of significant percentages of the face-centered cubic (FCC) phase. Furthermore, the increase of Cl^- ions concentration led to an increase of residual deformations in the crystalline structure of cobalt deposits, while the increase of SLS and boric acid concentrations led to a decrease of these residual deformations.

https://doi.org/10.1007/s11663-024-03098-y

I. INTRODUCTION

COBALT is a strategic metal mostly used in the production of batteries, super alloys, catalysts and other industrial chemicals. Its supply depends on the global economic scenario of nickel (Ni) and copper (Cu) since 95 pct of cobalt is a by-product of Cu and Ni mining.[1,2] The world's largest exporter of cobalt concentrates is the Democratic Republic of Congo. However, in terms of high-value-added cobalt production, China has been the leader over the last few years, importing around US$2.23 billion of cobalt in 2018.[3,4] This fact was due to the manufacture of rechargeable batteries for electric vehicles (EVs).

During the last decade cobalt demand reached historic levels due to the growing production of rechargeable batteries for electric vehicles.[1–3] According to the site *Trading Economics*,[5] in the first trimester of 2018 cobalt prices reached a peak at 95,250 US$/t. After a drop, and oscillation around 30,000US$/t from 2019 to 2021, cobalt prices rose again in 2022 reaching 82,596 US$/t. According to *Cobalt Institute*,[4] cobalt alloys/superalloys correspond to 21 pct of the total world cobalt production, while the rechargeable batteries correspond to 57 pct. Military and aerospace industries are responsible for boosting the global cobalt production.[6] Other applications of metallic cobalt include vehicles manufacturing, magnets and metallic coatings.[6,7]

DANIELLE COSTAL DE CASTRO, PEDRO PAULO MEDEIROS RIBEIRO, and ACHILLES JUNQUEIRA BOURDOT DUTRA are with the Programa de Pós-Graduação em Engenharia Metalúrgica e de Materiais, COPPE, Universidade Federal do Rio de Janeiro (UFRJ), Av. Horácio Macedo, 2030, Cidade Universitária, Rio de Janeiro, RJ 21941-914, Brazil. Contact e-mail: danielle.costal@coppe.ufrj.br IRANILDES DANIEL DOS SANTOS is with the Instituto Tecnológico Vale (ITV), Rua Prof. Paulo Magalhães Gomes, s/n, Morro do Cruzeiro, Ouro Preto, MG 35400-000, Brazil. REINER NEUMANN is with the Centro de Tecnologia Mineral (CETEM), Av. Pedro Calmon 900, Cidade Univrsitária, Rio de Janeiro, RJ 21941-596, Brazil.

Manuscript submitted January 17, 2024; accepted April 12, 2024.
Article published online April 29, 2024.

Electrowinning is the main route for metallic cobalt production and the reduction of operational costs allied to the yield of good quality deposits is a challenge faced by the industries throughout the time. This issue is due to the simultaneous side reaction of hydrogen evolution, whose presence can affect current efficiency, specific energy consumption and deposits morphology.[1,8] Most of the papers on cobalt electrowinning report the effects of varying current density, pH, temperature and concentration on electrorecovery with the aim of improving the conditions of cobalt electrowinning.[9–13] Defining these parameters is necessary, but not sufficient, to optimize the process. To avoid problems caused by interferers, strategies such as the introduction of additives were adopted, which can change several physical and chemical properties of metallic cobalt, such as microhardness, average grain and crystallite sizes, crystalline phases, growth structure and morphology. However, there are gaps to be filled due to the lack of published research on the use of different types of additives.

The study of the influence of organic and inorganic additives on current efficiency responses, specific energy consumption, morphology and crystallographic orientation has been the main area of research for the advancement of cobalt electrowinning process.[9–17] In the literature, some authors investigated the influence of organic surfactant additives (saccharin, tetramethylammonium bromide, butenediol, sodium gluconate, *etc.*) on the microstructure, morphology, hardness and crystallographic orientation of cobalt deposits.[18] According to Jeffrey *et al.*,[14] the presence of 5 g L^{-1} of sodium lauryl sulfate reduces the generation of hydrogen at low overpotentials and improves the morphology of the deposited metallic cobalt. Lu *et al.*,[12] reported a reduction of the surface tension on cobalt deposits with the addition of sodium lauryl sulfate.

The hydrogen evolution during cobalt electrowinning is one of the main factors that affect the appearance and properties of the deposits. The formation of dendritic Co deposits favors the formation of hydrogen bubbles, mainly on the sides of the metallic deposits and dentrites tips, due to the uneven current distribution on these areas.[12,19–21] The irregular grains formed are responsible for generating punctual defects, such as gaps or interstitials, in which impurity atoms can occupy empty spaces. This negatively affects the purity and quality of the cobalt deposit.[22–25] Alternatively, boric acid in cobalt electrolyte solutions, due to its buffer effect, prevents the formation of hydroxides at the electrode/solution interface and, consequently, prevents a possible incorporation of some cobalt hydroxy-complexes at the cathode.[26]

Das and Subbaiah[27] pointed out that a boric acid concentration of 10 g L^{-1} in the electrolyte increased current efficiency to 86 pct and also improved the appearance of the deposit, however in a concentration of 40 g L^{-1} it led to a reduction of current efficiency to 80 pct. In deeper study, by Tripathy *et al.*,[28] no influence of boric acid on current efficiency and crystallographic orientation was observed in cobalt sulfate solutions. On the other hand, Juma[18] investigated the influence of boric acid in ionic liquids on the electrowinning of cobalt and an increase of the cobalt deposit hardness, from 382 HV to 455 HV, was observed in the presence of approximately 37 g L^{-1} of this additive.

Regarding chloride ions, Pradhan *et al.*,[15] and Castro *et al.*,[19] verified changes in the surface morphology and structure of the deposits, in addition to the change of orientation in the crystalline planes during the electrodeposition process. Pradhan *et al.*,[15] observed that the introduction of 5 g L^{-1} of chloride ions affected the orientation of cobalt crystallites, resulting in more homogeneous surfaces. According to Castro *et al.*,[19] some cobalt complexes, formed with the chloride ion, such as $CoCl^{+}$, in the electrolyte solution, can be reduced on the cathode. For low concentrations of chloride ions (1.0 to 5.0 g L^{-1}) in cobalt sulfate solution, the preferential formation of two cationic species, Co^{2+} and $CoCl^{+}$, was indicated.

In the present study, authors aim to show the influence of the additives boric acid, sodium lauryl sulfate and chloride ion on current efficiency, specific energy consumption, morphology and physical properties of electrowon cobalt deposits. Although there are some articles in the literature addressing this topic,[10,15,18,28] this study presents an integrated approach with different methodologies and techniques (cyclic voltammetry and electrowinning tests allied to SEM, EDS, optical microscopy, XRD, microhardness) to obtain the results and coherent conclusions. The main properties investigated were morphology, hardness, growth structure, crystalline phases and grain and crystallite sizes. The scheme shown in Figure 1 illustrates the importance of this work. Cobalt electrodeposited from a solution with impurities can generate a material with coarse grain size, with many imperfections, which generates a fragile deposit (residual deformation), irregular, with low purity (solute atoms occupying gaps and interstices in the crystalline structure of the cobalt) and porous. The additives used are intended to enable the formation of a cobalt deposit with grain size, morphology and mechanical properties suitable for further processing and industrial applications.

II. MATERIALS AND METHODS

A. *Cyclic Voltammetry Tests with Cobalt Sulfate Solutions*

For the cyclic voltammetry tests, 10 different analytical grade cobalt sulfate heptahydrate solutions were prepared in 100 mL volumetric flasks, and the additive of interest at the desired concentration was added to each solution. The solutions were transferred to a 100 mL electrolytic cell. The variables temperature, pH, and cobalt concentration for voltammetry were kept constant, in accordance with previous work by Passos *et al.*[13] Thus, a cobalt sulfate solution with a concentration equal to 60 g L^{-1} of Co and pH 4 was transferred to a cell heated by a thermostatic bath at a temperature of 60 °C. A single additive was added to each of these solutions at a certain concentration, as shown in Table I.

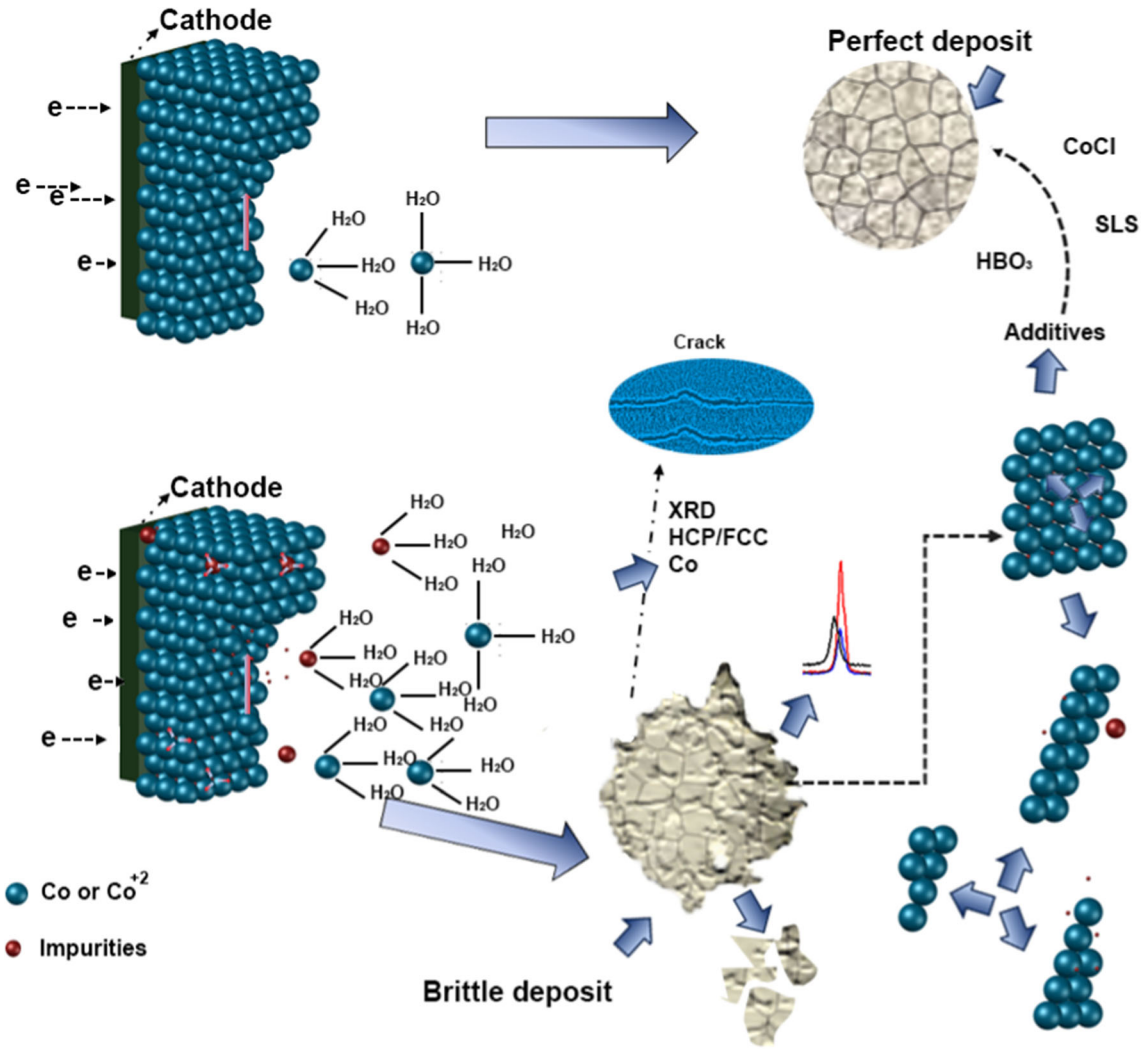

Fig. 1—Schematics of cobalt electrowinning in absence and presence of impurities. The presence of impurities makes cobalt deposits brittle. The addition of Sodium Lauryl Sulfate (SLS), boric acid (HBO_3), and cobalt chlorite (CoCl) improve the mechanical properties and morphology of cobalt deposits. Where *XRD* X-ray diffraction, *HCP* hexagonal close-packed, *FCC* Face-Centered Cubic, blue spheres = cobalt, red spheres = impurities (Color figure online).

Table I. Concentrations Range of Additives in Cobalt Sulfate Solution for Cyclic Voltammetry Tests

Additives Introduced in the Solution of $CoSO_4 \cdot 7H_2O$	Concentrations Range (g L^{-1})
Sodium Lauryl Sulfate (SLS)	0.02-0.05
H_3BO_3	10.0-50.0
$CoCl_2$	1.0-5.0

The cyclic voltammetry tests were carried out with a Metrohm Autolab® potentiostat coupled to an electrolytic cell, which was composed of the solution under study and three electrodes, namely the working electrode (AISI 304 stainless steel with 0.386 cm^2 of contact area), the counter electrode (Ti/RuO_2), separated by a horizontal distance of 2.5 cm from the working electrode, and the reference (Ag/AgCl/KCl 3M), which was placed close to working electrode.

The potential scanning rate for the voltammetric tests was 1 mV s^{-1} with initial and final potentials equal to 0.0 and − 0.6 V, respectively. The results were presented as graphs of current density (mA cm^{-2}) vs. potential (*E*).

B. *Electrowinning Tests in Cobalt Sulfate Solutions*

Cobalt electrowinning tests were carried out, in the presence of additives, with solutions of cobalt sulfate with a volume of 100 mL. The temperature was maintained at 60 °C, the initial pH at 4, the cobalt concentration at 60 g L^{-1} and the current density at 200 A m^{-2}, as described by Passos *et al.*[13] Each electrolyte solution received a specific condition, related to the type and concentration of the additive, as indicated in Table II. As a result, 10 different experiments were carried out in triplicate.

Table II. Additive Concentrations in $CoSO_4 \cdot 7H_2O$ Solution

Level	SLS (g L^{-1})	H_3BO_3 (g L^{-1})	$CoCl_2$ (g L^{-1})
Minimum (−)	0.02	10.0	1.0
Maximum (+)	0.10	50.0	5.0
Central Poit	0.05	30.0	3.0

The current efficiency of each test was determined through the ratio between the mass of the deposit and the theoretical mass, obtained in accordance with Faraday's law. Furthermore, the specific energy consumption (SEC) was calculated according to Eq. [1].

$$\mathrm{SEC} = I \cdot t \frac{V}{CE} \quad [1]$$

where V is the applied cell voltage and the product $I{\cdot}t$ is associated with the charge, according to Faraday's law, necessary to deposit 1 kg of cobalt, which is 909.4A h. The deposits mass was measured (after drying at 120 °C) with an analytical balance.

The morphology and purity of cobalt deposits were analyzed using scanning electron microscopy (SEM). The equipment used was a TESCAN®, model VEGA3, coupled to a BRUKER® energy dispersive spectroscopy (EDS). The macrographic images of the deposits were captured with the aid of an Avanscope® digital optical microscope.

The crystalline phases were determined by X-ray diffraction (XRD) with the Bruker-AXS D8 Endeavor equipment, under the following operating conditions: Co Kα radiation, λ = 0.15406 nm, generator operated at 40 kV and 40 mA, goniometer speed of 0.02 deg/s collected from 4 to 105 deg (2θ), with a LynxEye position sensitive detector. The softwares Diffrac.Eva, Diffrac.Topas, and the PDF2+ database were used to identify and quantify the different metallic phases. The analysis of crystallographic orientations was based on spherical harmonic parameters. The width at half height was measured from the diffractograms obtained by XRD and with the aid of the Topas software through the use of the peak shaping function. The size of the crystallites was calculated from Eq. [2].[29]

$$D = \frac{k\lambda}{\beta \cos\theta} \quad [2]$$

where D is the crystallite size, k is the constant dependent on the shape of the crystallites, λ is the incident wavelength, β is the width of the peak at half height and θ is the Bragg angle.

To determine the grain size of the deposits, each sample was polished using a sequence of 320, 600 and 2500 grit sandpaper. Then, it was then polished with a 6, 3 and 1 μm diamond paste. To reveal the contours of the microstructure, an acid attack was carried out using a 200 mL aqueous solution with 4 g of picric acid and 4 grams of ferric chloride.

The microhardness of cobalt metallic deposits was measured with a microhardness meter applying the Vickers method and calculated from Eq. [3].[30] The load used was 0.300 kgF.

$$\mathrm{HV} = \frac{1854P}{d} \quad [3]$$

where HV is the hardness, P is the load in kgF and d is the average length of the diagonals of the diamond projection dent transformed to millimeters.

The samples were analyzed micrographically, and the captured images were added to the ImageJ®[31] image analysis software in order to determine the grain size by determining the size of the deposits' grain boundaries and its average area. For the measurement to be representative, it was necessary to carry out a minimum of 50 measurements from one contour edge to the other.

III. RESULTS AND DISCUSSION

A. *Influence of Additive Concentrations on Cyclic Voltammetry Tests*

The voltammetric graphs obtained by the technique were crucial to analyze the cathodic behavior of cobalt in a sulfate solution with additives, identifying the crossover potential, the onset of cobalt ions reduction and the polarization behavior of each additive.

1. *Influence of sodium lauryl sulfate (SLS)*

The effect of SLS concentration on the voltammograms is presented in Figure 2. It can be observed that the increase of SLS concentration in the solution led to a decrease of cathodic current density values during the cathodic scan, resulting in a consequent decrease of the Co^{2+} ions reduction rate, especially at concentrations greater than 0.02 g L^{-1}. Additionally, higher concentrations of this additive in solution displaced the onset potential of Co^{2+} ions reduction to more negative values. Consequently, the reduction of both H^+ and Co^{2+} ions, in the presence of the additive is simultaneously inhibited, as illustrated in Figure 2, which shows a decrease of current density during the cathodic scan with the increase of the additive concentration. In fact, Lu *et al.*,[12] observed that the addition of 5–20 mg L^{-1} of SLS in cobalt sulfate solutions resulted in smoother and more uniform deposits, reducing the defects on the metal surface caused by the adhesion of hydrogen bubbles on the deposit surface.

2. *Influence of boric acid*

The effect of boric acid concentration on voltammograms is shown in Figure 3. It is possible to verify that concentrations of 30 g L^{-1} and 10 g L^{-1} of boric acid in solution led to a decrease of the reduction rate of Co^{2+} and H^+ ions, since current density during the cathodic scan is decreased, while the concentration of 50 g L^{-1} polarized these reactions and displaced the onset of Co^{2+} ions reduction to more negative potentials, which

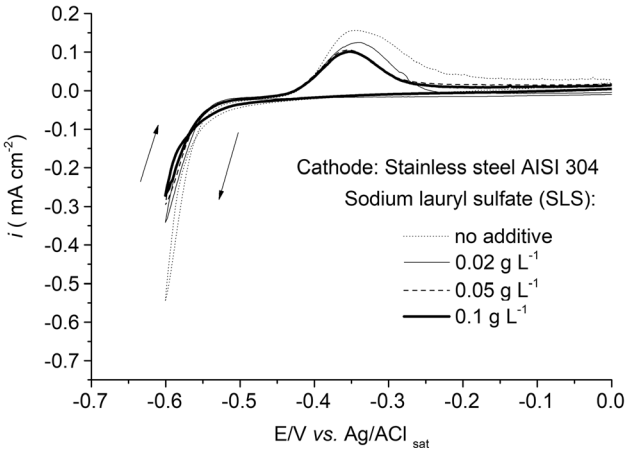

Fig. 2—Effect of SLS concentration on the voltammograms of cobalt sulfate solution with 60 g L^{-1} of Co Co^{2+} ions, at 60 °C, pH 4 and scan rate 1 mV s^{-1}.

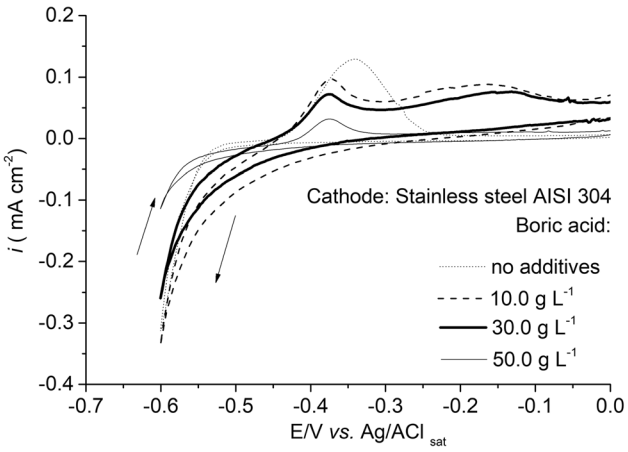

Fig. 3—Effect of boric acid concentration on voltammograms of cobalt sulfate solution with 60 g L^{-1} of Co^{2+} ions, at 60 °C, pH 4 and scan rate 1 mV s^{-1}.

is undesirable, since it demands more energy to reach the desirable current density and can favor hydrogen evolution.

According to Zhou *et al.*,[11] and Das and Subbaiah[27] boric acid is responsible for maintaining the pH of the electrode/solution interface neighborhood buffered, preventing its increase due to the reduction of H^+ ion concentration at the site and the possible formation of complexes such as $CoOH^+$. Castro *et al.*,[19] reported that the addition of boric acid to a cobalt sulfate solution in concentrations ranging from 10 to 70 g L^{-1} resulted in a shift of the onset potential for Co^{2+} ions reduction to more negative values at a scan rate of 20 $mV.s^{-1}$ and a potential scan range of 0.0 to -0.8 V.

3. *Influence of Cl^- ions*

The effect of chloride ion concentrations on the voltammograms is presented in Figure 4. It can be observed that chloride ions concentrations exceeding 1 g L^{-1} in the electrolyte solution resulted in a decrease of current density during the cathodic scan, leading to a

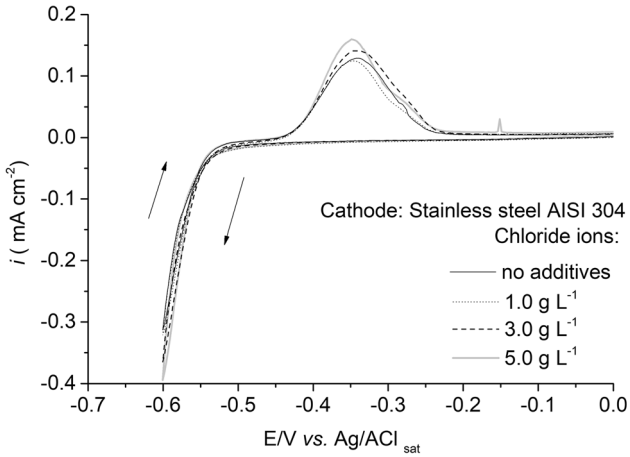

Fig. 4—Effect of Cl^- ions concentration on voltammograms of cobalt sulfate solution with 60 g L^{-1} of Co^{2+} ions, at 60 °C, pH 4 and scan rate 1 mV s^{-1}.

consequent reduction of the reduction rate of Co^{2+} ions. No significant change was observed of the onset potential for Co^{2+} ions reduction in the presence of Cl^- ions. This behavior was corroborated by Castro *et al.*,[19] in a previous work, in the presence of other additives, as, SLS, boric acid and sodium sulfate.

B. *Influence of Additives Concentration on Electrowinning*

The analysis of the influence of additives on the physical and chemical characteristics of the cobalt deposits produced by the electrowinning was based on the results of current efficiency, specific energy consumption, morphology, microhardness, deposit appearance, crystallographic orientation and grain and crystallite sizes of cobalt.

1. *Effect of additives on current efficiency and specific energy consumption*

The current efficiency and specific energy consumption results, along with their standard deviation values, for cobalt electrowinning are presented in Table III. The relative standard deviation values indicated a high level of reliability in the accuracy of the data, as they are within an acceptable analytical limit of relative error range below 4 pct.

It can be observed that the concentration of 0.05 g L^{-1} of SLS resulted in the highest current efficiency, 95.5 pct, and, simultaneously, the lowest specific energy consumption, 1.80 kWh kg^{-1}. However, the concentration of 0.1 g L^{-1} of SLS led to a drop in current efficiency to 94.5 pct and to an increase of the specific energy consumption to 1.82 kWh kg^{-1}. These observations indicated that the presence of this additive, in higher concentrations, can impair the electrowinning performance. Regarding the boric acid, an increase in its concentration up to 50 g L^{-1} resulted in a sharp decrease of the current efficiency and to an increase of the specific energy consumption to 87 pct and 2.08 kWh kg^{-1}, respectively, when compared to lower

Table III. Effect of Additives Concentrations on CE and SEC of Cobalt Electrowinning from a Sulfate Solution of $CoSO_4 \cdot 7H_2O$ with 60 g L^{-1} of Co^{2+} Ions at 60 °C, pH 4 and Current Density of 200 A m^{-2}

Concentration (g L^{-1})	CE Average (Pct)	SD (Pct)	SEC Average (kWh kg^{-1})	SD (Pct)	Cell Potential (Volts)
Pure Solution					
0.00	90.70	1.10	2.00	2	2.20
SLS					
0.02	94.10	0.78	1.83	3	1.85
0.05	95.50	1.97	1.80	4	1.84
0.10	94.60	1.31	1.82	3	1.85
Boric Acid					
10.00	92.50	1.08	1.88	3	2.00
30.00	91.80	1.77	1.91	4	2.00
50.00	87.10	0.50	2.08	1	2.00
Cl^- Ions					
1.00	92.30	0.94	1.87	1	2.00
3.00	94.10	0.86	1.83	2	2.00
5.00	94.20	0.78	1.87	3	2.00

concentrations of this additive. According to the studies by Tripathy *et al.*,[28] lower concentrations of boric acid (12 g L^{-1}) in solutions of cobalt sulfate led to an increase of current efficiency. This behavior suggests that at lower concentrations, the buffering effect of boric acid is more effective. On the other hand, the addition of Cl^- ions at concentrations up to 3 g L^{-1} resulted in an increase of current efficiency to 95.2 pct and a reduction of the specific energy consumption to 1.81 kWh kg^{-1}. As reported by Pradhan *et al.*,[15] the addition of Cl^- ions at concentrations up to 2 g L^{-1} did not promote significant changes in current efficiency values.

The analysis of the influence of additives on the morphology of cobalt metal deposits was conducted through macroscopic observations, considering the deposits aspect and structure. The Macrographs of cobalt deposits generated under the influence of different additives concentration are presented in Figure 5.

It is evident that the additives SLS and boric acid modified the appearance of cobalt deposits. For SLS, the addition of up to 0.05 g L^{-1} (Figure 5(c)) led to more uniform, smother, and clear deposits. However, for higher concentrations, the formation of imperfections at the edges of the deposits was observed. Regarding the boric acid, the increase of its concentration to 50 g L^{-1} reduced the size of imperfections of the deposits, but not their quantity, as illustrated in Figure 5(g), where the presence of a lot of pinholes can be observed. Concerning the introduction of Cl^- ions, no significant macroscopic modifications were observed in the deposits. As emphasized by Pissolati[32] organic compounds play a fundamental role in reducing the imperfections of nickel deposits, promoting the formation of more uniform deposits. In the context of SLS, concentrations up to 0.05 g L^{-1} provided its effectiveness as surfactant, minimizing the adherence of hydrogen bubbles on the deposit surface and, consequently, the occurrence of pits.

C. *Effect of Additives on the Chemical and Physical Properties of Deposits*

1. *Scanning electron microscopy (SEM) and energy dispersive spectroscopy (EDS)*

The influence of additives on the structure of cobalt deposits was evaluated by scanning electron microscopy as presented in Figure 6.

In Figure 6, the presence of cracks in the cobalt deposits with the addition of boric acid and Cl^- ions is noticeable. Under all conditions, there was a refinement in the grain size of the deposits compared to the pure cobalt sulfate condition.

The effect of additives concentrations on the cobalt structure is presented in Figure 7. The SEM images of cobalt deposits in the presence of SLS indicated a decrease of crack formation with increasing concentrations of SLS (Figures 7(a) and (b)). On the other hand, the addition of boric acid at minimum and maximum concentrations (Figures 7(c) and (d)) showed an increase of cracks quantity. Castro *et al.*,[19] and Juma *et al.*,[18] reported that deposits formed in the presence of high boric acid concentrations (50 and 40 g L^{-1}, respectively) exhibited small voids uniformly distributed throughout the deposit layer. These voids were attributed to the additive acidity and to hydrogen evolution. Regarding the influence of Cl^- ions on cobalt deposits (Figures 7(e) and (f)), an increase in its concentration reduced the quantity of cracks in the deposits. The presence of cracks in cobalt deposits may be related to several factors such as the presence of dissolved hydrogen in the metal lattice due to a pH drop during the electrolysis, the deposition of hydroxide layers on the cobalt layers due to the presence of intermediate hydroxylated species, which are pH dependent, at the electrode/solution interface, and to the presence of the harder hexagonal close-packed phase.

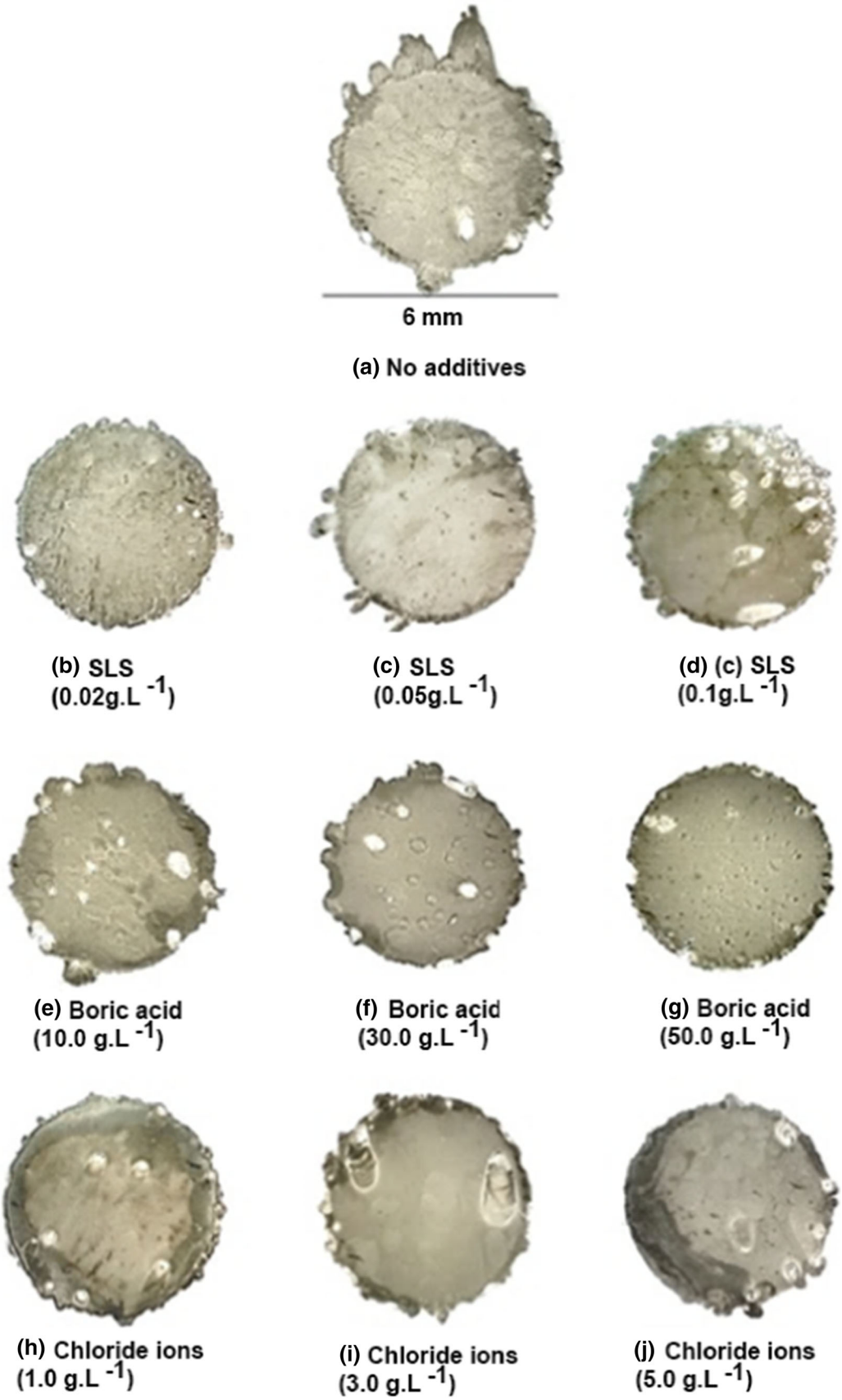

Fig. 5—Influence of additives concentrations on the morphology of cobalt deposits obtained by electrowinning with an electrolytic cell with 100 mL of cobalt sulfate solution with 60 g L^{-1} of Co^{2+} ions, at 60 °C and pH 4.

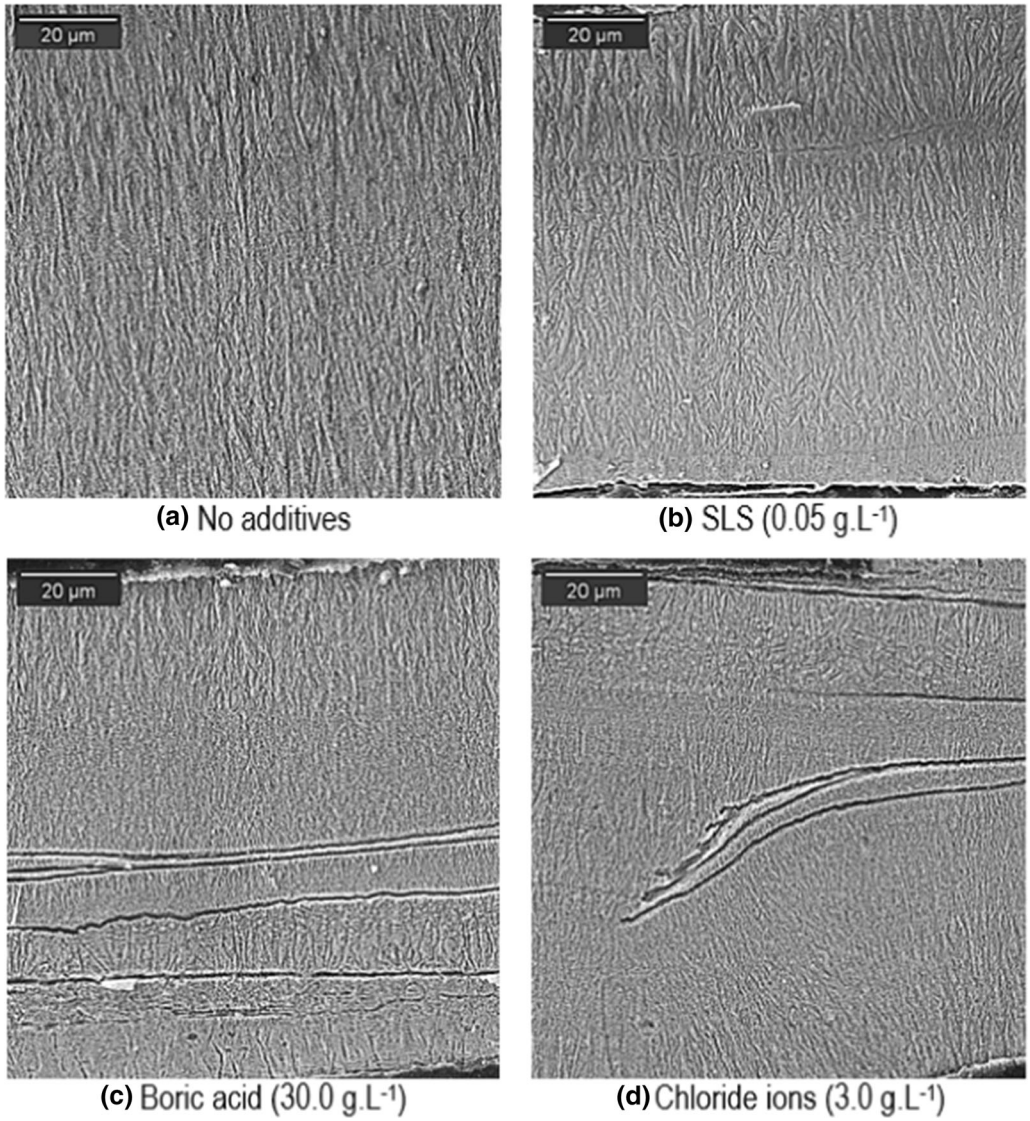

Fig. 6—Cross section of electrowon cobalt deposits from cobalt sulfate solutions in the presence of different additives. Current density of 200 A m^{-2}, Co^{2+} ions concentration of 60 g L^{-1}, at 60 °C and pH 4.

During cobalt electrowinning, hydrogen penetrates in the metal structure in its atomic form, and due to its small atomic volume, it can rapidly diffuse into the crystal lattice, even at relatively low temperatures, causing the formation of cracks. A significant portion of the produced atomic hydrogen tends to combine into its molecular form, being released as gas bubbles. The absorption capacity of hydrogen in metals can occur through the formation of hydrides.[33] However, it is evident that additives have an impact on the morphology and structure of cobalt. For example, the introduction of boric acid results in an increase in the quantity of cracks, while increasing concentrations of SLS and Cl^- ions tends to decrease them.

The composition of the deposits close to the cracks can provide valuable information about their origin, since hydroxide and oxide complexes can be formed due to the pH increase at the electrode/solution interface as a result of hydrogen evolution. Figure 8 presents an EDS mapping of the deposits close to the cracks, in the presence of each additive in order to identify the presence of oxygen near the cracks, which would be an indicative of hydroxide/oxide formation during deposition.

A higher concentration of oxygen in the cobalt deposits was observed near the cracks, as shown in Figure 8. This suggests the presence of hydroxide/oxide complexes that may had been incorporated into the deposit as layers during the 6 hours of electrolysis. As a result, the material becomes more susceptible to cracks due to composition variations during its formation. Fayette *et al.*,[34] indicated that the absorption of hydrogen atoms at grain boundaries and interstitial sites in the crystalline structure can cause cracks in the metallic deposits due to tensile stresses. Additionally, Matsushima *et al.*,[35] reported that the adsorption of colloidal cobalt hydroxide can generate residual stresses in the deposits, which, in turn, may be responsible for

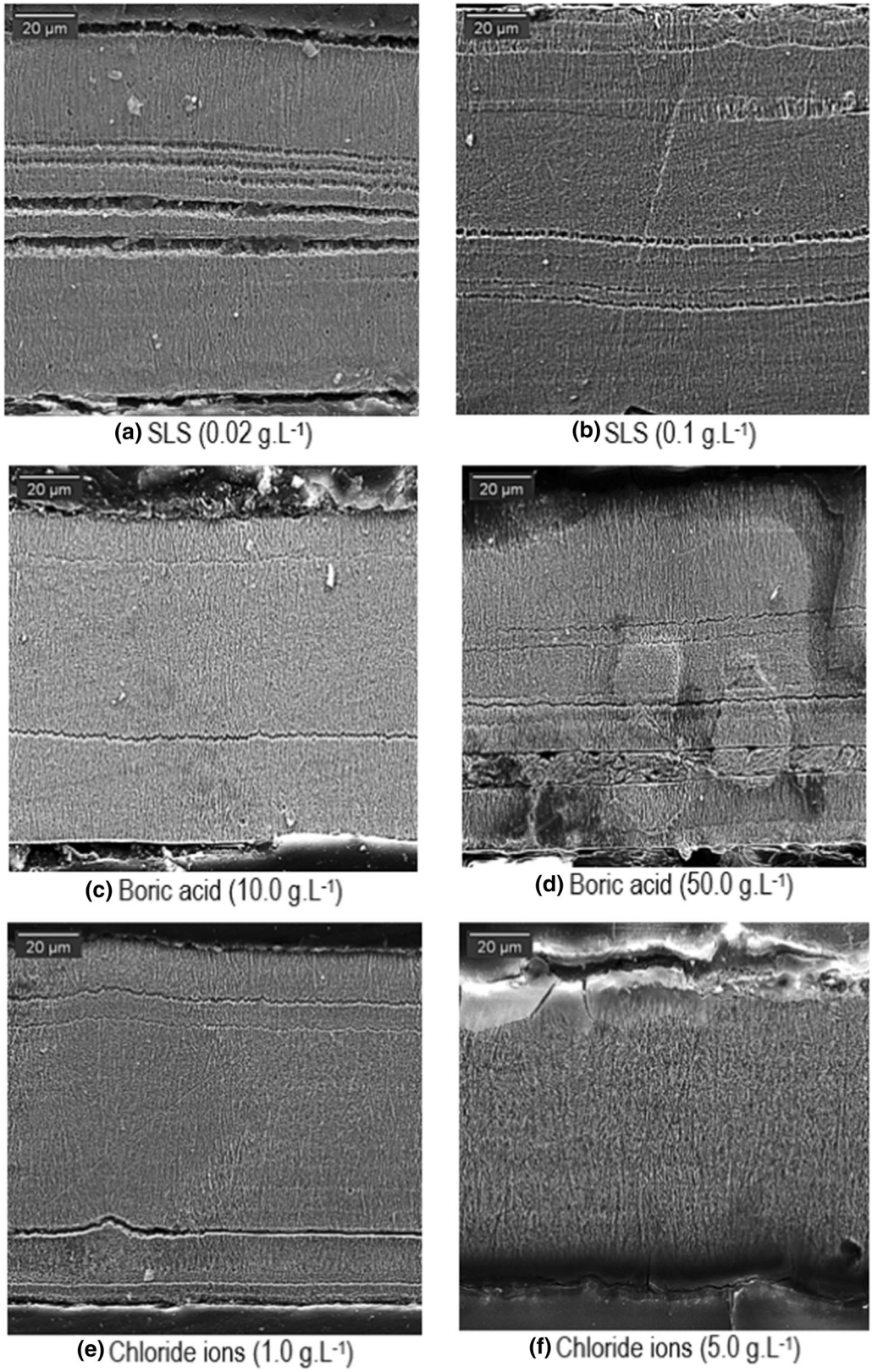

Fig. 7—Cross section of electrowon cobalt deposits from cobalt sulfate solutions in the presence of different additives concentrations (minimum and maximum concentration of additives). Current density of 200 A m^{-2}, Co^{2+} ions concentration of 60 g L^{-1}, at 60 °C and pH 4.

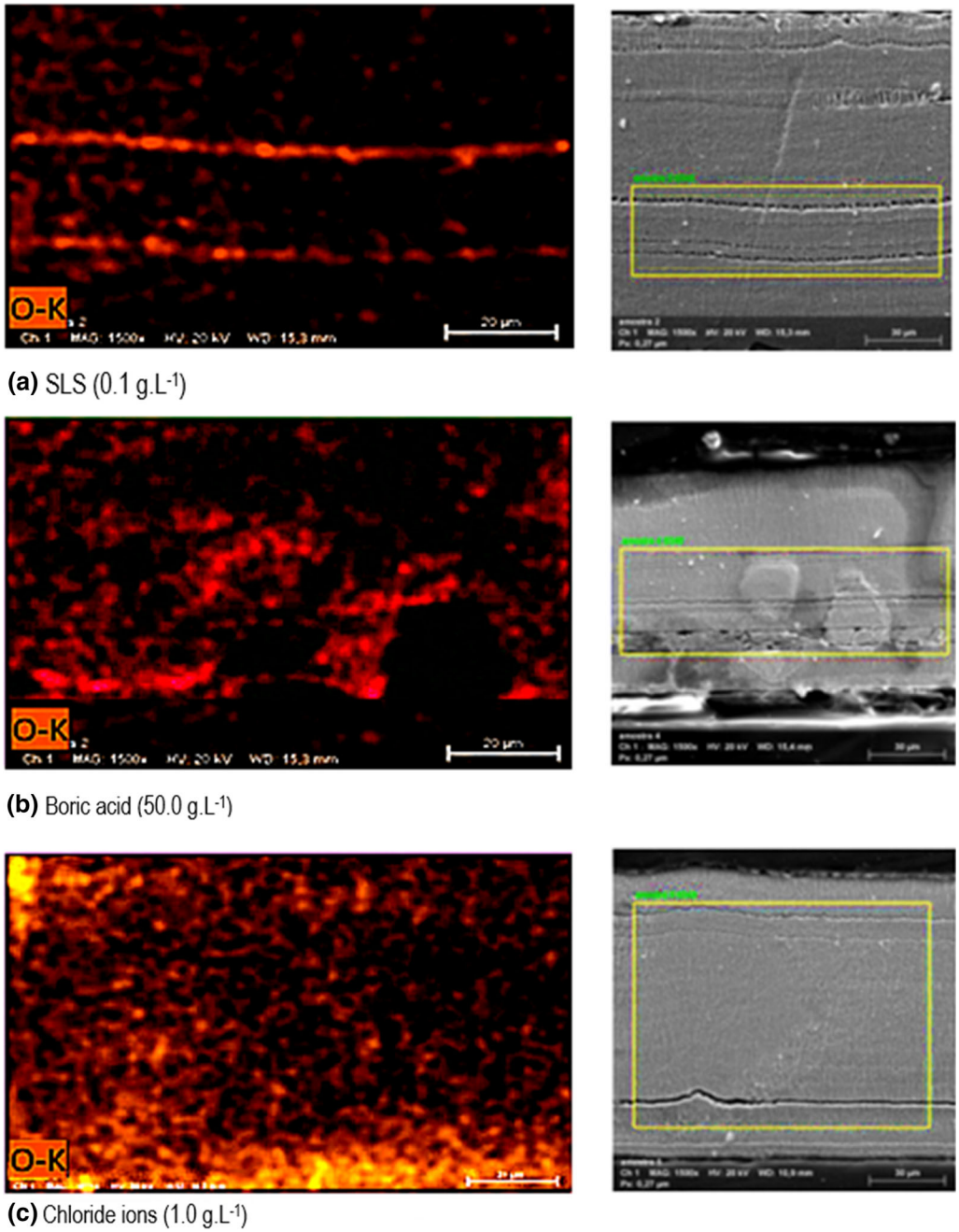

Fig. 8—EDS area mapping of cobalt deposits in the presence of different additives in a cobalt sulfate solution with current density of 200 A m^{-2}, 60 g L^{-1} of Co^{2+} ions, at 60 °C and pH 4. Magnification: 2000x. Focused on oxygen detection.

the crack formation. Santos *et al.*,[36] reported that $Co(OH)_2$ can be formed simultaneously with Co deposits at a temperature of 48 °C and pH 5.

Figure 9 presents EDS line scans of cobalt deposits aiming at verifying which elements are present near the crack locations in the cobalt deposits produced with different additives concentrations. It is possible to observe oxygen peaks in the deposits obtained with the presence of SLS and boric acid. For the latter, the oxygen peak is more evident and closer to the crack, where the cobalt counting drops.

2. *Percentage of crystalline phases and average sizes of cobalt crystallites and grains*

Table IV presents the preferred orientations and crystalline phases, along with their quantification, of electrowon cobalt from sulfate solutions with different additives concentrations, obtained by X-ray diffraction.

According to Table IV, the predominant crystalline phase of cobalt deposits is hexagonal compact (HCP). However, the increase of SLS and Cl^- ions concentration led to the formation of a small percentage of the face-centered cubic (FCC) crystalline phase.

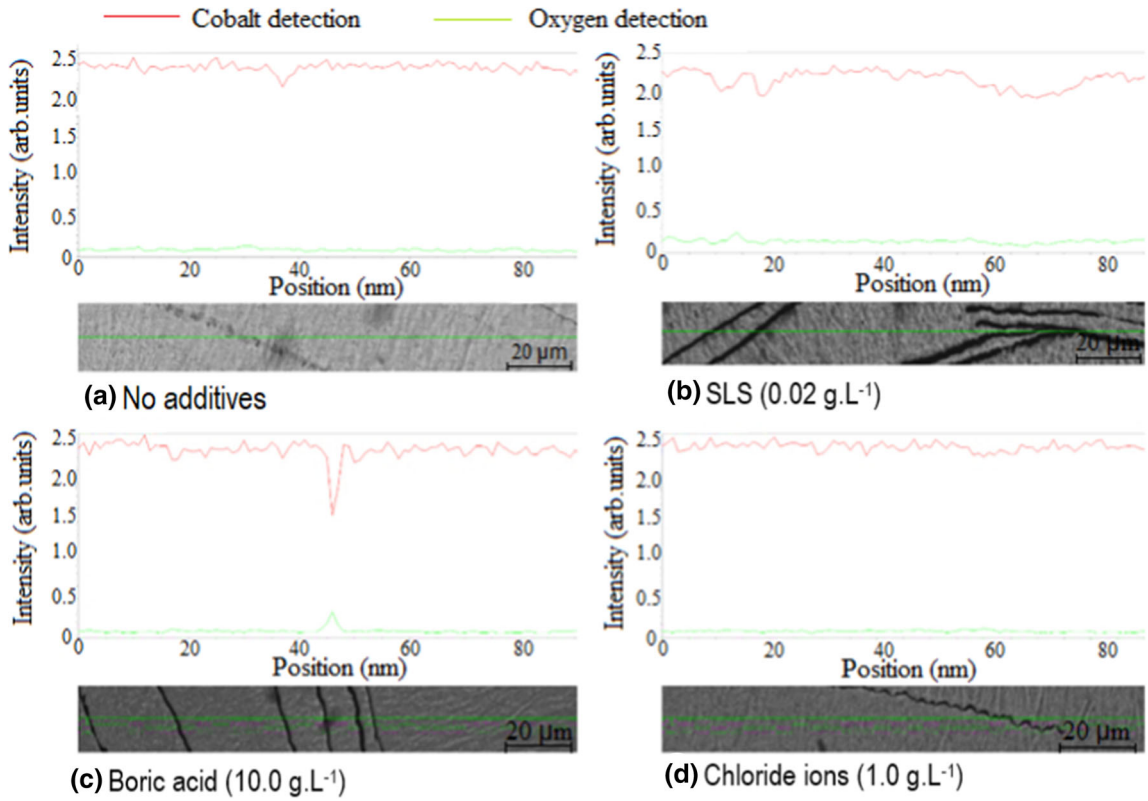

Fig. 9—EDS line scanning of cobalt deposits obtained in the presence of different additives from a cobalt sulfate solution with a current density of 200 A m^{-2}, 60 g L^{-1} of Co^{2+} ions, at 60 °C and pH 4. Red line: cobalt. Green line: oxygen. Magnification: 2000x. Focused on oxygen detection (Color figure online).

Table IV. Effect of Additive Concentrations on Crystallographic Orientation and Crystalline Phases in a Cobalt Deposit of $CoSO_4 \cdot 7H_2O$ with 60 g L^{-1} of Co^{2+} Ions at 60 °C and pH 4

Additives	Concentration (g L^{-1})	Crystallographic Orientation	Crystalline Phases (Pct)
Pure Solution	—	(100)(002)(101)	HCP (100 pct) FCC (0 pct)
SLS	0.02	(100)(002)(101)	HCP (86 pct) FCC (14 pct)
	0.05	(100)(002)(101)	HCP (88 pct) FCC (12 pct)
	0.10	(100)(002)(101)	HCP (87 pct) FCC (13 pct)
Boric Acid	10.0	(100)(002)(101)	HCP (100 pct) FCC (0 pct)
	30.0	(100)(002)(110)	HCP (100 pct) FCC (0 pct)
	50.0	(100)(002)(101)	HCP (100 pct) FCC (0 pct)
Cl^- Ions	1.0	(100)(002)(101)	HCP (100 pct) FCC (0 pct)
	3.0	(100)(002)(101)	HCP (100 pct) FCC (0 pct)
	5.0	(100)(002)(101)	HCP (81 pct) FCC (18 pct)

The diffractograms of cobalt for different concentrations of SLS, boric acid, and Cl^- ions are presented in Figures 10, 11, and 12. It can be observed that the presence of SLS, boric acid, and Cl^- ions modified the cobalt diffraction peaks intensity compared to deposits obtained from pure cobalt sulfate solutions. In the tests without the use of additives or in the presence of boric acid only, a preferred orientation was observed in the plane with a peak at 41.6 deg (100), while in the presence of SLS and Cl^- ions, the preferred orientation occurred at the peak located at 44.3 deg (002—HCP and 111—FCC). Furthermore, it is possible to observe that the increase of SLS and boric acid concentrations led to an increase of cobalt diffraction peaks intensity located at 44.3 deg. The same intensity profile of the curves was observed at 41.6 deg. Thus, the increase of these additive concentrations led to a decrease of residual deformations and, consequently, a decrease of residual stress values. For the addition of Cl^- ions, it was observed that a higher concentration led to a reduction of the preferential peak intensity located at 44.3 deg. Thus, the presence of Cl^- ions led to an increase of the deposit's residual deformation. This decrease is characteristic of non-uniform residual deformations.[37] Moreover, there is a displacement to the right of all peaks of the cobalt obtained in the presence of additives, when compared to standard deposits. These displacements are characteristic of uniform compressive deformations.[38]

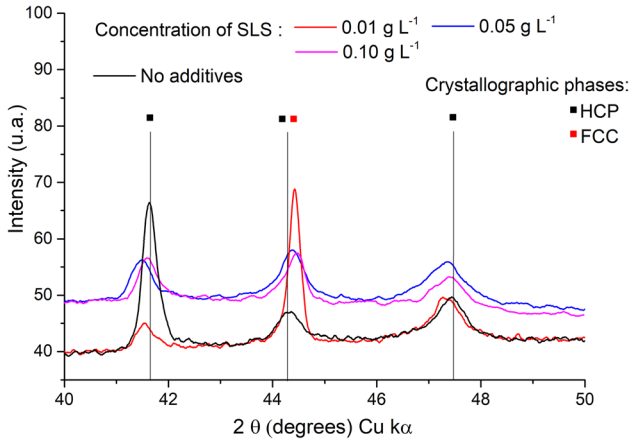

Fig. 10—Effect of SLS concentration on the orientation of cobalt crystallographic phases.

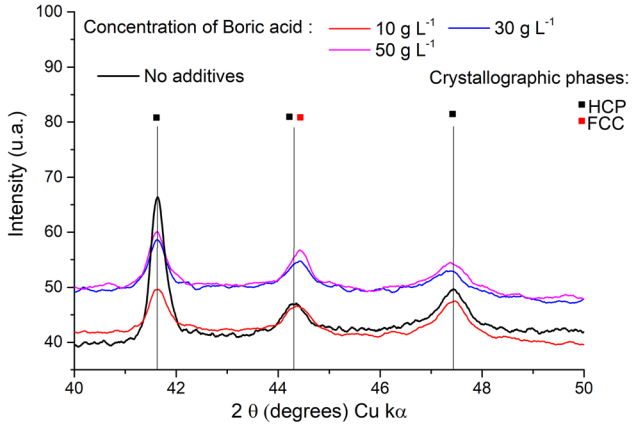

Fig. 11—Effect of boric acid concentration on the orientation of cobalt crystallographic phases.

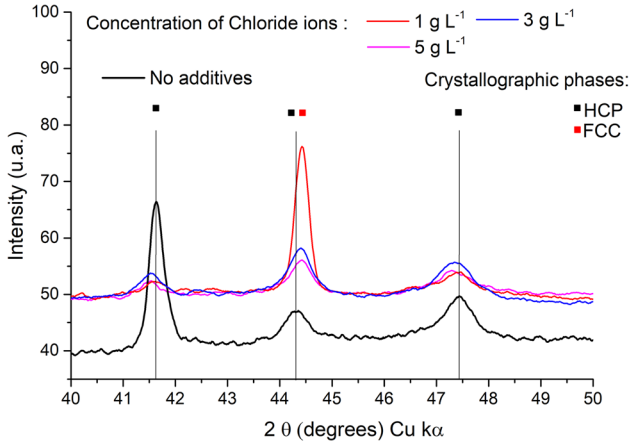

Fig. 12—Effect of Cl^- ions concentration on the orientation of cobalt crystallographic phases.

In addition to the analysis of crystalline phases, the average size of crystallites was calculated using the Scherrer equation [Eq. 2]. The effect of additives on the cobalt crystallites size at different concentrations is presented in Figure 13.

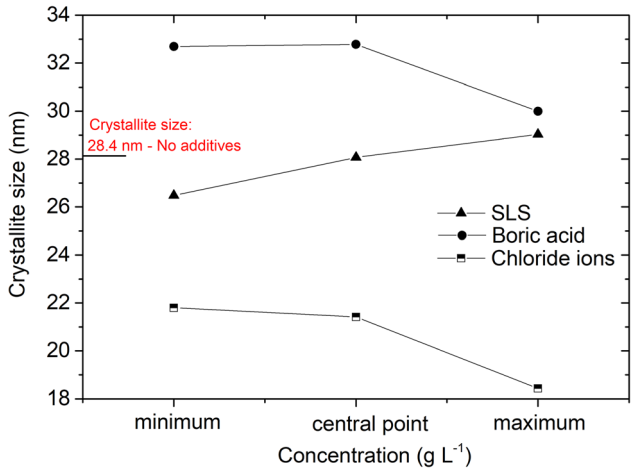

Fig. 13—Effect of additive concentrations on the average size of cobalt crystallite.

The presence of 1 g L^{-1} of Cl^- ions led to a significant change of the crystallites average size, compared to those obtained from the pure solution, resulting in a decrease of crystallite size by more than 21.42 pct with this additive. However, the presence of SLS and boric acid produced larger crystallite sizes, compared to the pure solution. The presence of SLS at a concentration of 0.02 g L^{-1} led to the formation of crystallites with a smaller average size (26 nm) than that obtained from the pure solution (28 nm).

The additives influence directly the average size of the crystallites as they do with the cobalt ions reduction as well. Thus, late electroreductions (initiation of reduction at more negative potentials) led to the formation of larger crystallites sizes. Castro *et al.*,[19] reported that elevated concentrations of SLS and boric acid displaced the onset of cobalt electroreduction in sulfate solutions to more negative potentials.

The additives can influence the size of crystallites of cobalt deposits and consequently certain physical properties, such as average grain size and microhardness. The influence of additive concentrations on the average grain size of cobalt deposits is presented in Figure 14.

From the metallographic images of cobalt deposits, it can be observed that the presence of 1 g L^{-1} of Cl^- ions promoted a significant change in the average grain size compared to those obtained from the pure solution. On the other hand, the presence of SLS tended to generate slightly larger grains with increasing concentrations, while in the presence of boric acid the grains size tend to be much larger as its concentration is increased.

The estimated values of the average grain size of cobalt under the influence of additives and their concentrations is presented in Table V.

It is evident that the presence of boric acid presents a remarkable effect on cobalt grain size. At concentrations of 30 and 50 g L^{-1} an increase of the cobalt average grain size to 35.58 and 44.07 μm, respectively was observed. On the other hand, SLS presented only a tiny effect on the cobalt grain size. The presence of 5.0 g L^{-1} of Cl^- ions led to a significant change of the average grain size compared to those obtained from the pure

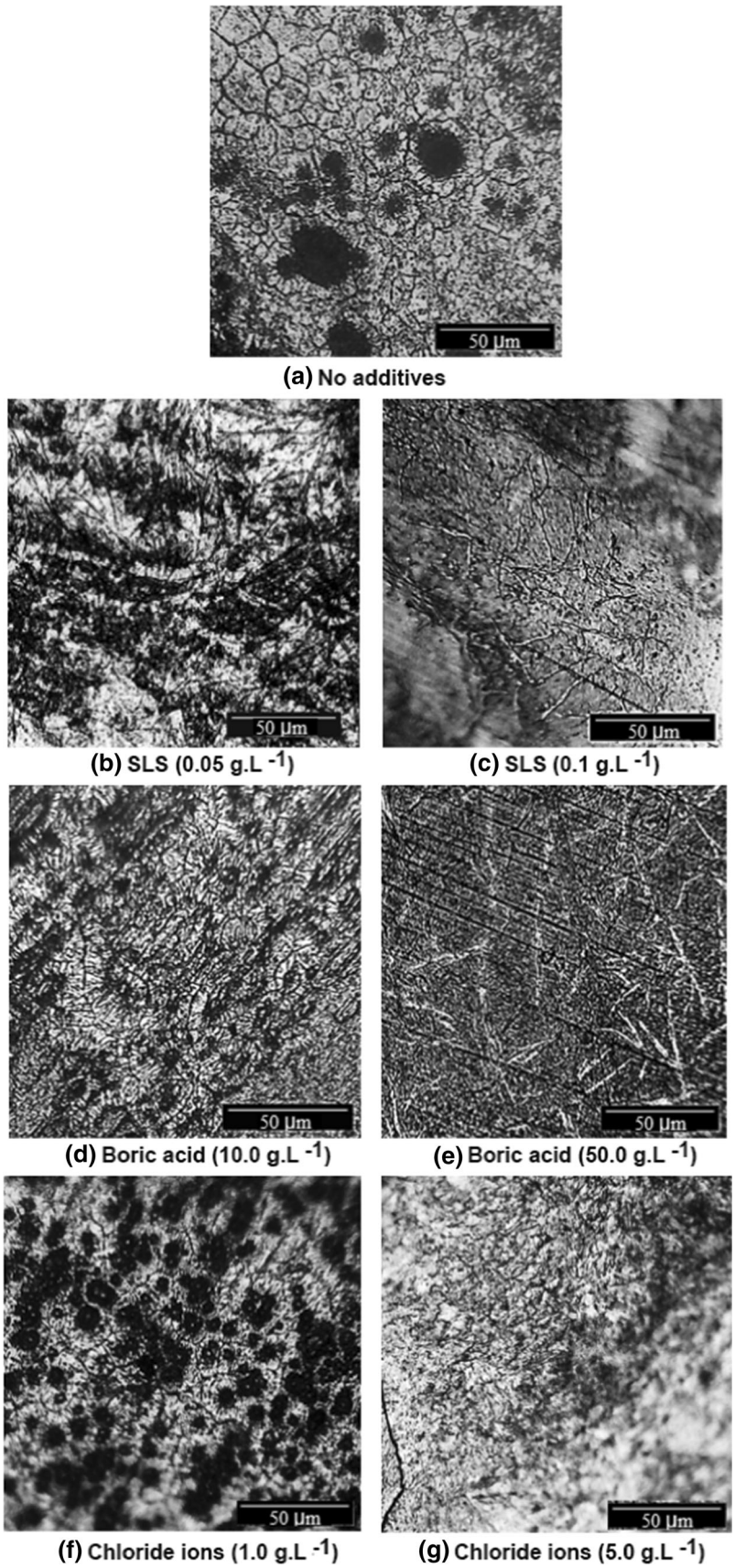

Fig. 14—Cobalt deposits metallography obtained in the presence of different of additives concentration. Magnification: ×200. Metallography image scale: 50 μm.

Table V. Effect of Additives Concentration on the Average Grain Size of Cobalt Deposits Produced from a Solution of $CoSO_4$ with 60 g L^{-1} of Co^{2+} Ions at 60 °C and pH 4

Average Cobalt Grain Size Without Additives: 23.42 μm					
SLS (g L^{-1})	Grain size (μm)	Boric acid (g L^{-1})	Grain size (μm)	Ions chloride (g L^{-1})	Grain size (μm)
0.02	20.39	10.0	22.12	1.0	19.01
0.05	19.16	30.0	35.58	3.0	17.94
0.1	21.41	50.0	44.07	5.0	9.19

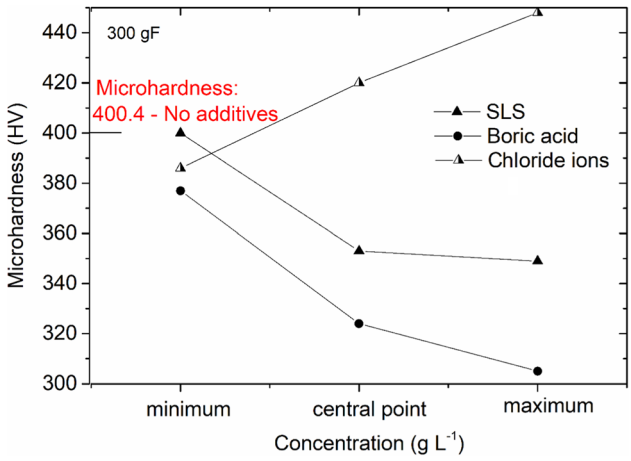

Fig. 15—Effect of additive concentrations on the microhardness of cobalt deposits.

solution (23.42 μm), reaching a value of 9.19 μm. The presence of Cl^- ions affected the concentration of electroactive species in the solution, as cobalt complexes with Cl^- can be formed and reduce cobalt activity in sulphate solutions.[39] Furthermore, it is important to emphasize that the average size of cobalt crystallites followed the same trend of their average grains size obtained under the influence of additives.

3. *Microhardness of cobalt deposits*

The effect of additives concentration on the microhardness of cobalt deposits is presented in Figure 15. Deposits formed with the addition of Cl^- ions at concentrations higher than 1 g L^{-1} exhibited higher microhardness values compared to deposits generated from the pure solution. For example, in Figure 15, it can be observed that in the presence of 5 g L^{-1} of Cl^- ions a deposit with a microhardness of 450 HV was obtained, while from the pure solution, the microhardness was 400.4 HV. On the other hand, in the presence of 10 g L^{-1} of boric acid, a decrease of microhardness to 380 HV was observed. The boric acid concentration of 50 g L^{-1} led to an even more reduction of microhardness (300 HV). The introduction of SLS in solution also decreased the microhardness values of the deposits; for instance, the addition of 0.1 g L^{-1} reduced the microhardness value to 345 HV.

The analysis of microhardness results under the influence of additives corroborated the values obtained by the Scherrer equation for the average size of crystallites. The higher concentration of Cl^- ions in solution led to increased hardness and a smaller average crystallites size, while the presence of SLS and boric acid resulted in an increase of the average crystallites size and lower microhardness values. The hardness change can be attributed to the decrease of grains size, which increase grains boundary, hindering the movement of dislocations due to the increase of barriers.

D. *Cobalt Electrowinning Considerations*

Other factors previously discussed in the introduction of this article influence the cobalt electrodeposition and the physicochemical properties of the deposits, such as temperature, current density, cobalt concentration, and pH variations during electrolysis. There is a variety of well-established articles in the literature that address those factors.[9–13,36,39] The effect of pH variation during electrolysis is crucial since prolonged electrolysis can lead to a decrease in pH. Thus, there is a need for pH control in the electrolytic solution, as a sharp pH decrease can lead to a more intense hydrogen evolution on the cathode and its sorption in the deposits and, consequently leading to brittle deposits, which are subjected to warping, crack formation and eventually rupture. Another point to be considered is the formation of hydroxides at the cathode-solution interface, due to local pH increase caused by hydrogen evolution associated with high current densities, which can be incorporated into the cobalt deposits. The pH variation during electrolysis in bench scale tests, can be buffered through the increase of solution volume associated with the same cathode area. For pilot scale or industrial electrolysis in a continuous flow circuit, a tank with cobalt hydroxide slurry should be included in the circuit to neutralize the acid generated on the anode and at the same time to reestablish cobalt ions concentration. The authors are conducting further research to assess the degradation of additives and their impact on cobalt deposit formation, based on pH variation, during longer-term electrolysis. A reduction of the edge effect of the deposits and absence of cracks have already been observed with decreasing pH variation through the increase of solution volume. However, it is important to consider that the introduction of additives into the cobalt electrolyte solution based on the conditions established by this research improves the appearance and properties of cobalt deposits. It is believed that this behavior should also occur in larger-scale tests. Additionally, there is a grain refinement and an increase of microhardness when chloride ions are added to the solution. Therefore, the production of high-purity

cobalt on an industrial scale requires pH control associated with controlled additives concentration, the latter being poorly explored by industries and available literature.

IV. CONCLUSIONS

The results of the analyses in this study contributed to the optimization of various industrial applications of cobalt. The proper concentration of the additives SLS, boric acid, and Cl^- ions, enabled the formation of a cobalt deposit with appropriate grain size, morphology, and mechanical properties for the processing and industrial applications of the metal.

Cyclic voltammetry indicated that higher concentrations of SLS, boric acid, and Cl^- ions led to an increase of the overpotential of cobalt deposition.

In the electrowinning tests with a cobalt sulfate solution, conducted in a 100 mL-cell, the addition of SLS, in a concentration of 0.05 g L^{-1}, led to the highest current efficiency, 95.5 pct and to the lowest specific energy consumption, 1.80 kWh kg^{-1}. On the other hand, the increase of boric acid concentration resulted in a decrease of current efficiency and an increase of the specific energy consumption.

Macroscopic images of the cobalt deposits indicated that the presence of SLS at a concentration of 0.05 g L^{-1}, was beneficial to deposit morphology.

Cross section images of the deposits obtained by SEM showed significant differences of the structure of the deposits in the presence of additives. The increase of boric acid concentration led to an increase of the number of cracks in the deposits, while the increase of SLS concentration resulted in a reduction of the cracks. On the other hand, the higher concentration of Cl^- ions led to the formation of deposits without the presence of cracks. EDS mapping indicated an accumulation of oxygen near the cracks location, indicating the possibility of the presence of hydroxy/hydroxyl compounds in the cobalt deposits.

X-ray diffraction results indicated that the predominant crystalline phase was hexagonal close-packed (HCP). However, an increase of the face-centered cubic (FCC) phase percentage was observed with the increase of Cl^- ions concentration. The average crystallites and grains sizes decreased with the presence of Cl^- ions. On the other hand, the addition of boric acid and sodium lauryl sulfate led to an increase of the crystallite size. The measurement of the average grain size of cobalt under the influence of additives followed the same trend of the average crystallite size. The different intensity of the cobalt deposit's diffraction peaks in the absence and presence of additives indicated the possibility of residual deformation in the deposits obtained in the presence of additives.

The highest concentration of Cl^- ions produced a deposit with highest hardness, reaching a value of 450 HV. The deposit formed from the pure solution presented a hardness of 400 HV. On the other hand, the highest concentration of boric acid produced deposits with the lowest hardness, approximately 300 HV.

ACKNOWLEDGMENTS

The authors would like to acknowledge Instituto Tecnológico Vale (ITV), CNPq and Coordenação de Aperfeiçoamento de Pessoal de Nível Superior – Brasil (CAPES) for the support. In addition, this study was financed in part by the Coordenação de Aperfeiçoamento de Pessoal de Nível Superior – Brasil (CAPES) – Finance Code 001.

CONFLICT OF INTEREST

On behalf of all authors, the corresponding author states that there is no conflict of interest.

REFERENCES

1. P.A. Dias, D. Blagoeva, C. Pavel, and N. Arvanitidis: *Publ. Off. Eur. Union*, 2018, vol. 10, p. 97710.
2. M. Li and J. Lu: *Science*, 2020, vol. 367, p. 979. https://doi.org/10.1126/science.aba9168.
3. T. Zhang, Y. Bai, X. Shen, Y. Zhai, C. Ji, X. Ma, and J. Hong: *Int. J. Life Cycle Assess.*, 2021, vol. 26, p. 1198. https://doi.org/10.1007/s11367-021-01925-x.
4. Cobalt Institute, 2021, *State of the cobalt market report*. https://www.cobaltinstitute.org/resource/state-of-the-cobalt-market-report-2021.
5. Cobalt Commodity, 2023, *Trading Economics*. https://pt.tradingeconomics.com/commodity/cobalt.
6. H. Hao, X. Sun, Z. Liu, F. Zhao, and J. Song: *Resour. Conserv. Recycl.*, 2019, vol. 149, p. 45. https://doi.org/10.1016/j.resconrec.2019.05.009.
7. U.S. Geological Survey, 2018, Mineral Commodity Summaries 2018, *United States Geological Survey*. https://minerals.usgs.gov/minerals/pubs.
8. C. Stinn and A. Allanore: *Electrochem. Soc. Interface*, 2020, vol. 29, p. 44. https://doi.org/10.1149/2.f06202if.
9. C. Lupi and D. Pilone: *Min. Eng.*, 2001, vol. 14, p. 1403. https://doi.org/10.1016/s0892-6875(01)00154-6.
10. J.H. Huang, C. Kargl-Simard, and A.M. Alfantazi: *Can. Metall. Q.*, 2004, vol. 43, p. 163. https://doi.org/10.1179/cmq.2004.43.2.163.
11. J. Zhou, S. Wang, and X.T. Song: *Nonferr. Metal Soc.*, 2016, vol. 26, p. 1706. https://doi.org/10.1016/s1003-6326(16)64279-6.
12. J. Lu, D. Dreisinger, and T. Glück: *Hydrometallurgy*, 2018, vol. 178, p. 19. https://doi.org/10.1016/j.hydromet.2018.04.002.
13. F.A.C. Passos, I.D. Santos, and A.J.B. Dutra: *Miner. Process. Extr. Metall. Rev.*, 2022, vol. 44, p. 481. https://doi.org/10.1080/08827508.2022.2095561.
14. M.I. Jeffrey, W.L. Choo, and P.L. Breuer: *Min. Eng.*, 2000, vol. 13, p. 123. https://doi.org/10.1016/s0892-6875(00)00107-2.
15. N. Pradhan, P. Singh, B.C. Tripathy, and S.C. Das: *Min. Eng.*, 2001, vol. 14, p. 775. https://doi.org/10.1016/s0892-6875(01)00072-3.
16. P. Patnaik, S.K. Padhy, B.C. Tripathy, I.N. Bhattacharya, R.K. Paramguru, and T. Nonferr: *Metal Soc.*, 2015, vol. 25, p. 2047. https://doi.org/10.1016/S1003-6326(15)63814-6.
17. S. Sudibyo, L. Hermida, and P.A. Reswari: *J. Mater. Sci. Appl. Energy*, 2021, vol. 10, p. 49.
18. J.A. Juma: *Arab. J. Chem.*, 2021, vol. 14, p. 103036. https://doi.org/10.1016/j.arabjc.2021.103036.
19. D.C. Castro, I.D. Santos, M.B. Mansur, and A.J.B. Dutra: *J. Braz. Chem. Soc.*, 2023, vol. 34, p. 1360.
20. F. Su, C. Liu, Q. Zuo, P. Huang, and M. Miao: *Mater. Chem. Phys.*, 2013, vol. 139, p. 663.
21. E.H. Moradi, K. Jafarzadeh, S. Borji, and H. Abbaszadeh: *Miner. Eng.*, 2015, vol. 77, pp. 10–16. https://doi.org/10.1016/j.mineng.2015.02.012.
22. D.F. Suarez and F.A. Olson: *J. Appl. Electrochem.*, 1992, vol. 22, p. 1002. https://doi.org/10.1007/BF01029577.

23. I.G. Sharma, P. Alex, A.C. Bidaye, and A.K. Suri: *Hydrometallurgy*, 2005, vol. 80, p. 132. https://doi.org/10.1016/j.hydromet.2005.08.003.
24. E. Peek, T. Akre, and E. Asselin: *JOM*, 2009, vol. 61, p. 43. https://doi.org/10.1007/s11837-009-0151-2.
25. Q. Song, Y. Zhao, C. Wang, H. Xie, H. Yin, and Z. Ning: *Hydrometallurgy*, 2019, vol. 189, 105111https://doi.org/10.1016/j.hydromet.2019.105111.
26. E.C. Pereira, F. Trivinho-Strixno, and J.S. Santos: *Surf. Coat. Technol.*, 2010, vol. 205, p. 2585. https://doi.org/10.1016/j.surfcoat.2010.10.005.
27. S.C. Das and T. Subbaiah: *J. Appl. Electrochem.*, 1987, vol. 17, p. 675. https://doi.org/10.1007/BF01007801.
28. B.C. Tripathy, P. Singh, and D.M. Muir: *Metall. Mater. Trans. B*, 2001, vol. 32B, p. 395. https://doi.org/10.1007/s11663-001-0023-9.
29. B.D. Cullity and S.R. Stock: *Elements of X-Ray Diffraction*, 3rd ed. Prentice Hall, Upper Saddle River, NJ, 2001.
30. A.C. Fischer-Cripps: *Solid Mech. Appl.*, 2014, vol. 203, p. 53. https://doi.org/10.1007/978-94-007-6919-9_3.
31. ImgeJ®, Schneider, C. A., Rasband, W. S., & Eliceiri, K. W.: *Nat. Methods*, 2012, vol. 9(7), pp. 671–75. https://doi.org/10.1038/nmeth.2089.
32. N.C. Pissolati and D. Majuste: *Hydrometallurgy*, 2018, vol. 175, p. 193. https://doi.org/10.1016/j.hydromet.2017.11.012.
33. V. Gentil, Corrosão, 4nd ed, v.1., Rio de Janeiro, LTC, 2003.
34. M. Fayette, U. Bertocci, and G.R. Stafford: *J. Electrochem. Soc.*, 2016, vol. 163, p. 146. https://doi.org/10.1149/2.0511605jes.
35. J.T. Matsushima, F. Trivinho-Strixino, and E.C. Pereira: *Electrochim. Acta*, 2006, vol. 51, p. 1960. https://doi.org/10.1016/j.electacta.2005.07.003.
36. J. Santos, R. Matos, F. Trivinho-Strixino, and E. Pereira: *Electrochim. Acta*, 2007, vol. 53, p. 644. https://doi.org/10.1016/j.electacta.2007.07.025.
37. A. Boumaiza, M. Bouras, and V.J. Rouag: *Theoret. Appl. Fract. Mech.*, 2012, vol. 61, pp. 51–56. https://doi.org/10.1016/j.tafmec.2012.08.006.
38. I.C. Noyen and J.B. Cohen: Residual Stress Measurement by Diffraction and Interpretation, *Materials Research and Engineering (MATERIALS)*, Springer. *N. Y.*, 1987. https://doi.org/10.1007/978-1-4613-9570-6.
39. O. Kongstein, G. Haarberg, and J. Thonstad: Current efficiency and kinetics of cobalt electrodeposition in chloride acid solutions. *Part II: The Influence of Chloride and Sulphate Concentrations, J. Appl. Electrochem.*, 2007, vol. 37, p. 675. https://doi.org/10.1016/10.1007/s10800-007-9298-0.